# Towards a two-process model of antisaccades in Parkinson's disease

J Lewis[1*], A Cope[2], S James[1], A Blenkinsop[1], S Anderson[3], K Gurney[1]

*1 Department of Psychology, University of Sheffield, UK*
*2 Department of Computer Science, University of Sheffield, UK*
*3 Automatic Control & Systems Engineering, University of Sheffield, UK*

* Correspondence: jen.lewis@sheffield.ac.uk, Western Bank, Sheffield, S10 2TN, UK.

## 1. Introduction

The antisaccade task involves generating a saccade in the opposite direction to a stimulus presented in the visual periphery. Successful performance of the task is believed to require two separate processes. First, an inhibitory process that suppresses an automatic saccade towards the stimulus. Second, a voluntary saccade generation process, which in turn involves an internal remapping of the visual saccade target and the execution of a saccade towards the internally generated target.

Correctly performed antisaccades have longer reaction times than prosaccades, typically taking 50-150ms longer to be initiated than automatic prosaccades. They are also more error-prone, with healthy controls making erroneous prosaccades towards the target on 5-30% of antisaccade trials, depending on the task design [1]. Parkinson's disease patients, however, make more errors on the antisaccade task, and take longer to generate a correct antisaccade, when compared with age-matched controls [2]. This impaired cognitive performance has been shown even in early-stage Parkinson's patients, despite the generally accepted notion that early-stage Parkinson's exclusively affects motor control [3].

Where Parkinson's disease is primarily a disorder of basal ganglia (BG) function via the loss of dopamine in striatum, patients' impairment on the antisaccade task points to the involvement of BG in the successful performance on the task. However, most computational modelling of the antisaccade task has focussed on the role of superior colliculus. Only one existing model of antisaccades includes BG [4]. This model, while novel and revealing, cannot fully account for the processes driving performance on the antisaccade task for two main reasons. Firstly, it has no antisaccade-related activation before the presentation of the visual target, whereas there is a large body of evidence suggesting that successful performance of an antisaccade relies primarily on the pre-setting of a fronto-parietal network in the period *before* the stimulus appears [5,6]. Secondly, depletion of dopamine in the model – the hallmark of Parkinson's disease – does not result in Parkinson's-like performance.

In the present work, we build on an existing model of the oculomotor system including basal ganglia to begin addressing these issues.

## 2. Materials and Methods

We use an existing model of the oculomotor system developed by Cope and colleagues [7]. The model uses rate-coded leaky integrator neurons, and comprises topographical representations of the main regions of the oculomotor system, including superior colliculus, frontal eye fields (FEF) and oculomotor BG. It has been shown to perform reactive prosaccades with accurate reaction times [7].

We introduce additional regions to the model to support the antisaccade task. First, a visual parietal basal ganglia-thalamocortical loop, including representations of the left and right parietal eye fields (PEF). These neural regions have been shown to be important for programming saccades and are active before a successful antisaccade [5,6]. This loop exerts a top-down influence on the oculomotor loop via corticocortical and corticostriatal projections, and introduces a means of programming volitional saccades to the model. Second, a prefrontal cortex (PFC) representation, which allows additional top-down, task-based influences on both oculomotor and parietal loops, via corticocortical and corticosubthalamic projections. PFC has shown similar pre-stimulus activity before a successful

antisaccade and is believed to exert goal related influences on its downstream targets [5,6]. The model architecture is illustrated schematically in fig. 1.

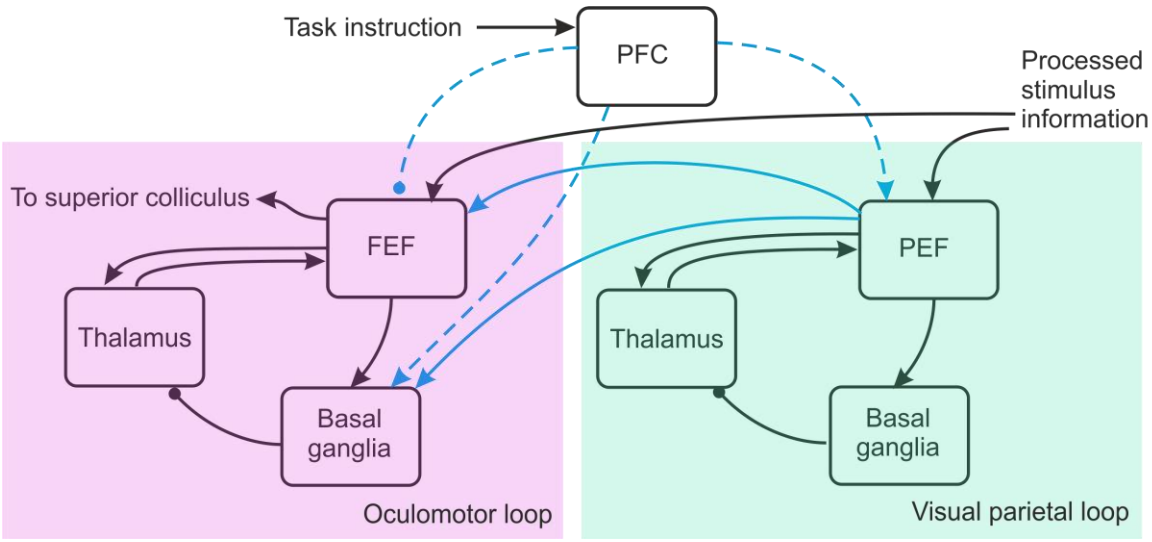


**Figure 1**. Overview of model architecture. The visual parietal loop (green region) has been added to the existing oculomotor loop (pink region), and further downstream nuclei (not illustrated). Arrowheads and filled circles indicate excitatory and inhibitory connections, respectively. Solid lines indicate topographic connections; dashed lines indicate diffuse connections. The antisaccade network influences oculomotor selection via connections highlighted in blue.

When activated by an antisaccade task instruction, PFC has two primary functional roles. It exerts an inhibitory influence on the oculomotor loop by exciting subthalamic nucleus (STN), raising the threshold for saccade initiation in BG output nuclei. It also sends low-level excitation to PEF, priming or 'pre-setting' the parietal BG loop for voluntary saccade generation.

After stimulus onset, PFC releases its inhibition of the oculomotor loop and its excitation of PEF. A leftward stimulus excites the right parietal visual hemifield, and vice versa, reflecting a remapped saccade command. Delays between stimulus onset and excitation of the remapped visual parietal areas are imposed to account for the necessary additional time for this process to occur. PEF subsequently excites the hemifield opposite to the stimulus location in the oculomotor loop, generating a competition between the stimulus-congruent (prosaccade) and stimulus-incongruent (antisaccade) saccade commands in FEF. This is resolved by the competitive selection processes within BG.

The model is implemented in the custom neural modelling software SpineML, using the SpineCreator interface [8] and simulated using BRAHMS [9].

## 3. Results

The model was tested in the antisaccade 'step' paradigm, using stimuli presented at 8° eccentricity. In the first simulation, PFC is successfully activated at fixation point onset. Here, this allows a low level of excitation to build up in PEF during the pre-stimulus period, and simultaneously makes a reactive prosaccade less likely by raising the selection threshold in BG via the excitation of subthalamic nucleus. Following stimulus onset, plus a delay reflecting visual processing time, pre-stimulus PFC activity is removed and activity in PEF begins to resolve according to the location of the stimulus. The resulting activation for the antisaccade location is propagated to FEF and oculomotor BG and is sufficient to successfully compete with the prosaccade location. An antisaccade is made at

approximately 300ms post-stimulus (fig. 2), consistent with human experiments showing that antisaccades are slower than prosaccades by about 50-150ms [1].

The third simulation shows the outcome of an antisaccade trial in which the fronto-parietal network does not engage. Here, PFC shows no activity during the pre-stimulus period and thus is unable to either inhibit automatic prosaccades or pre-set the relevant visual parietal areas. In this case, although activation of the parietal loop still occurs after stimulus onset, without the additional activation from

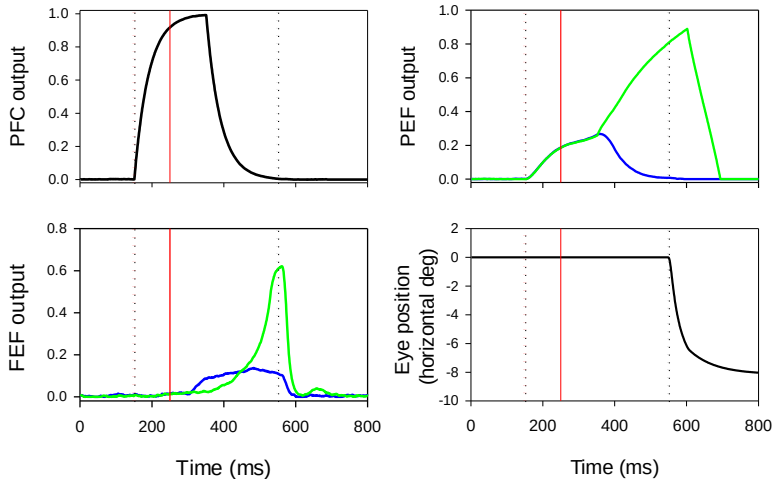


**Figure 2**. Output of key nuclei for successful antisaccade trial. PFC is the source of prestimulus activation in PEF, propagated to FEF allowing the antisaccade location to compete with the prosaccade location. A negative deflection in the horizontal eye position indicates a successful antisaccade. Green = antisaccade location neuron; blue = prosaccade location neuron. Red dotted = fixation onset; red solid = stimulus onset. Grey dotted = saccade initiation.

PFC this activation cannot build up soon enough to outcompete the automatic prosaccade command in the oculomotor loop. The result is a prosaccade with a latency of about 250ms (fig. 3); similar to that seen in standard prosaccade tasks, again consistent with experimental data.

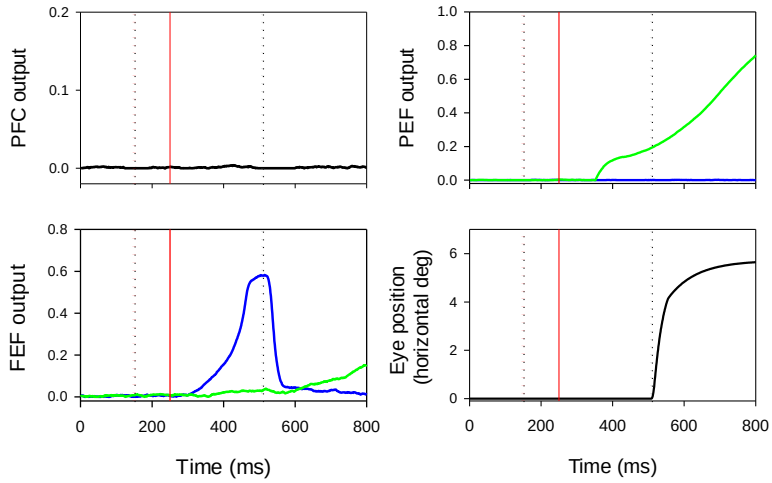


**Figure 3**. Output of key nuclei for unsuccessful antisaccade trial. PFC fails to activate in the prestimulus phase. In turn, PEF activity does not begin to build until well after stimulus onset. The resulting antisaccade command is thus unable to influence FEF before the prosaccade command is established. A positive deflection in the horizontal eye position indicates an error prosaccade. Traces as for fig. 2.

## 4. Discussion and Conclusions

We have presented the first computational model of antisaccades which relies on pre-stimulus processes in associative basal ganglia-thalamocortical loops to generate antisaccades. The model is able to produce correct prosaccades, correct antisaccades and error prosaccades with realistic latencies, and can thus begin to delineate the mechanisms by which pre-stimulus activity may be responsible for observed performance on antisaccade tasks.

Although this model is in its early stages, it shows significant promise in understanding the mechanisms by which antisaccades are generated in the healthy brain. Furthermore, the inclusion of simulated dopamine loss in multiple territories of BG will allow a thorough investigation of how this loss in Parkinson's disease may result in the observed higher error rates and slower antisaccade generation.

Future work will add a third, prefrontal BG loop, facilitating more realistic selection of task set. The addition of noise to the activation of this loop is expected to produce representative error rates in multiple trial simulations, as this should affect the onset time and ultimate magnitude of the pre-set signal originating in PFC.

We hypothesise that the reduction of simulated dopamine in the prefrontal loop should give rise to more errors, as prefrontal BG becomes less able to successfully select the necessary task representation to pre-set parietal areas for the programming of an antisaccade, accounting for the higher error rates observed in Parkinson's disease. Furthermore, the reduction of simulated dopamine in parietal areas should make the programming of such antisaccades more difficult, accounting for the observation of longer latencies on correct antisaccades in Parkinson's disease.

## 5. References


1. Hutton SB & Ettinger U, Psychophysiology. 2006; 43:302-13
2. Amador SC et al., Neuropsychologia. 2006; 44:1475-82
3. Antoniades CA et al., Movement Disord. 2015; 30(6):843-47
4. Wiecki TV & Frank MJ, Psychol. Rev. 2013; 120(2):329-55
5. Brown MRG et al., J Neurophysiol. 2007; 98:1751-62
6. Cameron IGM et al., NeuroImage. 2012; 60:1156-70
7. Cope A et al., Submitted to PLoS One
8. Richmond P et al., Neuroinformatics. 2014; 12(2):307-23
9. Mitchinson B et al., Adv Eng Inform. 2010; 24(1):49-61


## Acknowledgements


This work is partially funded by the EC FP7 project NoTremor- Virtual, Physiological and Computational Neuromuscular Models for the Predictive Treatment of Parkinson's Disease, Grant Agreement No. 610391